Analysis of Proton-Nucleus Scattering at 9.8 Mev*†

A. E. GLASSGOLD, W. B. CHESTON, M. L. STEIN, S. B. SCHULDT, AND G. W. ERICKSON
School of Physics, University of Minnesota, Minneapolis, Minnesota

(Received January 17, 1957)

Studies of nuclear scattering from an arbitrary complex central potential have been initiated. This first report is devoted to the analysis of proton-nucleus scattering at 9.8 Mev using the Saxon potential. Qualitative rules for the dependence of the cross section on the parameters of this model are presented for medium-heavy elements. An important feature of the analysis is that more than one set of optical model parameters is possible at this energy. These multiple solutions have in common approximately the same value of VR^2, where V is the real part of the nuclear potential and R is the interaction radius. This value does not differ significantly from the value used in the nuclear shell model. The imaginary part of the nuclear potential corresponds to an absorption length of about one nuclear radius.

I. INTRODUCTION

THIS is the first paper on an intensive study of nuclear scattering at intermediate energies from 10 to 100 Mev using the optical or complex potential model.[1–3] An important objective of this work is the determination in this energy range of the optical model parameters, i.e., the strengths of the real and imaginary parts of the nuclear potential and the size and shape of these potentials. The recent results[4,5] on the "electromagnetic" density of the nucleus and their contrast with the traditional nuclear radius emphasize the importance of the spatial dependence of the nuclear potential. Such differences, as well as an understanding of the real and imaginary parts of the nuclear potential from some more fundamental point of view, are important problems for nuclear dynamics.

The present report is particularly concerned with the analysis of Hintz's measurements of the elastic scattering of 9.8-Mev protons.[6] Reliable results can only be obtained with exact calculations of the scattering phase shifts. For this purpose a program was prepared for the Univac Scientific Computer[7] (E.R.A. 1103) to compute the nonrelativistic scattering from an arbitrary complex central potential. There are no restrictions on the masses or the charges of the colliding particles so that the scattering of neutrons and alpha particles can also be studied.[8] The potential energy consists of three terms,

$$V(r)=V_c(r)+Vf(r)+iWg(r). \quad (1)$$

The first term is the electrostatic potential and the latter two are the real and imaginary parts of the nuclear potential. In this program the radial dependence of each of these terms is completely arbitrary. The nuclear potential terms have been factored into strength parameters V and W and form factors $f(r)$ and $g(r)$ for the real and imaginary parts, respectively. Spin-orbit terms[9–11] are expected in Eq. (1), but their inclusion at this stage of the analysis would introduce more parameters into the model than the intermediate energy elastic scattering experiments could determine. This statement will be borne out by the results described later in this paper. The effects of the nuclear magnetic dipole and electric quadrupole moments are also ignored. In addition it is assumed that the "compound" elastic scattering[3] is negligible. Calculations of this type were first undertaken by LeLevier and Saxon[12] and Chase and Rohrlich[13] using square wells. Woods and Saxon[14,15] made the improvement of introducing rounded potential wells and subsequent work by Saxon and his associates[16,17] has achieved qualitative agreement with experiments at a number of energies.

In analyzing Hintz's experiments, the range of the optical model parameters for a particular potential was investigated in detail. As a consequence, it is possible to make some general qualitative statements about the dependence of the cross section on these parameters (Sec. II). These qualitative rules, together with a least-squares analysis, have been particularly useful in obtaining good agreement with experiment (Sec. III). An important result of this analysis is that more than one set of optical model parameters is possible at 10 Mev

* Supported in part by the U. S. Atomic Energy Commission.

† A preliminary report of this work was presented at the 1956 Thanksgiving meeting of the American Physical Society [Bull. Am. Phys. Soc. Ser. II, **1**, 339 (1956)].

[1] H. Bethe, Phys. Rev. **57**, 1125 (1940).

[2] Fernbach, Serber, and Taylor, Phys. Rev. **75**, 1352 (1949).

[3] Feshbach, Porter, and Weisskopf, Phys. Rev. **96**, 448 (1954).

[4] R. Hofstadter, Revs. Modern Phys. **28**, 214 (1956).

[5] K. W. Ford and D. L. Hill, *Annual Review of Nuclear Science* (Annual Reviews, Inc., Stanford, 1955), Vol. 5, p. 25.

[6] N. Hintz, preceding paper [Phys. Rev. **106**, 1201 (1957)]. This article contains a bibliography of other experiments on proton scattering.

[7] The authors are indebted to Remington Rand Univac for the use of their Univac Scientific Computer in St. Paul, Minnesota.

[8] A preliminary report on alpha-particle scattering has already been given by Cheston, Glassgold, Stein, Schuldt, and Erickson, Bull. Am. Phys. Soc. Ser. II, **1**, 339 (1956). A more detailed account is given in the following paper [W. B. Cheston and A. E. Glassgold, Phys. Rev. **106**, 1215 (1957)].

[9] E. Fermi, Nuovo cimento **11**, 407 (1954).

[10] W. Heckrotte and J. Lepore, Phys. Rev. **94**, 500 (1954).

[11] B. J. Malenka, Phys. Rev. **95**, 522 (1954).

[12] R. E. LeLevier and D. S. Saxon, Phys. Rev. **87**, 40 (1952).

[13] D. M. Chase and F. Rohrlich, Phys. Rev. **94**, 87 (1954).

[14] R. W. Woods, Ph.D. thesis, University of California at Los Angeles, 1954 (unpublished).

[15] R. W. Woods and D. S. Saxon, Phys. Rev. **95**, 577 (1954).

[16] Melkanoff, Moszkowski, Nodvik, and Saxon, Phys. Rev. **101**, 507 (1956).

[17] The authors would like to thank Dr. Saxon and Dr. Melkanoff for many helpful communications and discussions.

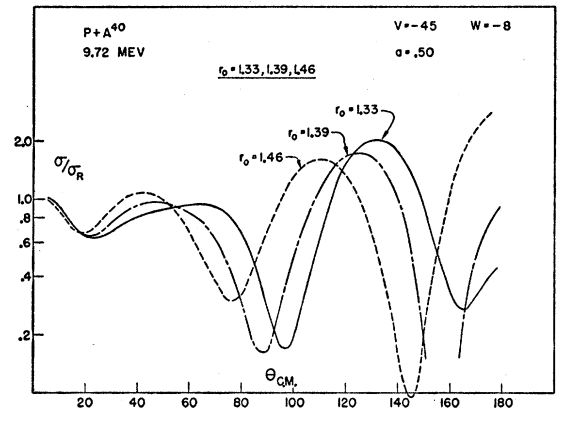

FIG. 1. Typical variation of elastic proton-nucleus scattering with nuclear radius. Increasing the radius shifts the diffraction pattern towards small angles.

for many cases. The solution most thoroughly studied is characterized by a nuclear radius midway between the traditional nuclear and electromagnetic values.

A brief discussion of the physical interpretation of the optical model parameters is given in Sec. IV. The details of the numerical calculations are summarized in the Appendix.

II. INVESTIGATION OF THE SAXON POTENTIAL

The first model studied intensively has been the one employed by Saxon and his associates.[14–17] This model uses the same form factor for the real and imaginary parts of the nuclear potential,

$$f(r)=\left\{1+\exp\left(\frac{r-R}{a}\right)\right\}^{-1}, \qquad (2)$$

and calculates the electrostatic potential from a uniform charge density of radius R. The above form factor has been used extensively in the analysis of electron scattering,[4] and it will be useful to relate the parameters in Eq. (2) with the "standard" electron scattering parameters, c and t. The first quantity, c, is the average radius, $\int_0^\infty dr f(r)$. The skin thickness, t, is the distance required for the form factor to drop from nine-tenths to one-tenth of its interior value. In the present case $c=R$; furthermore R also marks approximately the half-way point of the form factor, i.e., $f(R)\simeq\frac{1}{2}f(0)$ for $a\ll R$. The diffuseness a is related to the skin thickness t by the relation $t=4.40a$. The parameter r_0 will be used to specify the half-way radius R by the usual formula,

$$R=r_0A^{\frac{1}{3}}\times10^{-13}\text{ cm}. \qquad (3)$$

The radius R should be distinguished from the familiar radius R_s of the equivalent square well having the same root-mean-square radius. At 10 Mev the use of a continuous nuclear potential and a discontinuous square well for the charge density causes only very slight errors. The maximum difference in the electrostatic potential between a square well charge density and continuous charge density of the form in Eq. (2) is about 2%. Of course, the electrostatic potential for a uniform charge density is continuous.

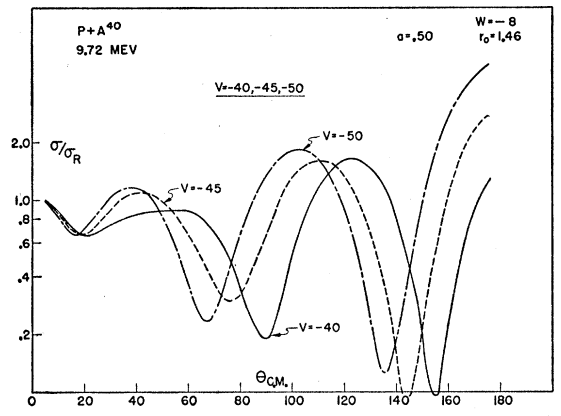

FIG. 2. Typical variation of elastic proton-nucleus scattering with the real part of the nuclear potential. Increasing the real part of the potential shifts the diffraction pattern toward small angles.

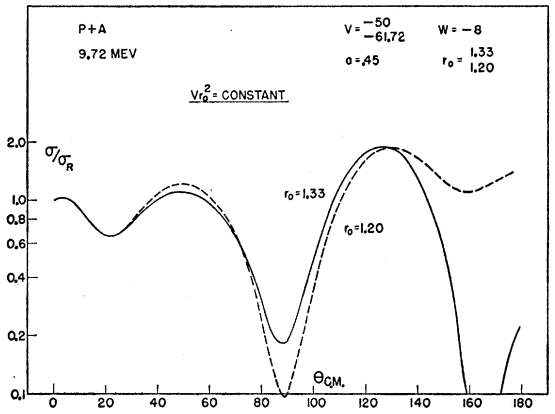

FIG. 3. Approximate stationary property of the maxima and minima in proton-nucleus scattering obtained by keeping VR^2 constant. In this case a and W were not changed while R^2 and V were changed by about 10%.

Preliminary to fitting any experimental data, a study was made of the dependence of the differential elastic scattering cross section on the parameters in this optical potential. These studies are illustrated in Figs. 1–5, which present ratios of the predicted scattering to Rutherford scattering for 9.72-Mev protons scattered from argon. These results are typical of medium and heavy elements. The results may be summarized in the following way:

1. The diffraction pattern is shifted towards smaller angles when V or R is increased.
2. Positions of maxima and minima are determined mainly by the value of VR^2.
3. The amplitude of the diffraction patters is damped when W is increased.

4. The diffraction pattern is shifted downwards by increasing a and, to a lesser extent, towards smaller angles.

The related effects of changing V and R, illustrated in Figs. 1 and 2, combine to give a stationary property to the maxima and minima when VR^2 is fixed.[18] This is illustrated in Fig. 3 where a change in R of about 10% is compensated by a change in V of about 20%; the values of a and W are the same. The facts that increasing V is equivalent to increasing R and that the positions of diffraction maxima and minima are determined by VR^2 show that a simple diffraction analysis, in which these positions are determined solely by the size of the nucleus, would be invalid.

The least reliable of the above rules is the last one dealing with changes in a, which is illustrated in Fig. 5. Sometimes the effect of increasing a is the same as increasing W, i.e., the minima are filled in and the maxima reduced. However, the main effect is usually a

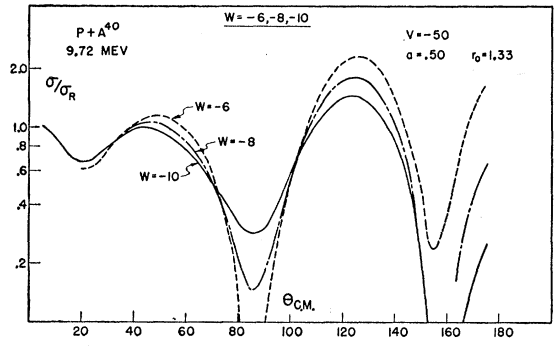

FIG. 4. Typical variation of elastic proton-nucleus scattering with the imaginary part of the nuclear potential for medium and heavy elements. The effect of increasing W is to damp the diffraction, i.e., to weaken both maxima and minima.

vertical shifting of the pattern. The associated effect whereby the pattern is also slightly shifted towards smaller angles can be understood in terms of an increase in some effective radius, such as the rms radius.

The qualitative statements just made must be treated with a great deal of caution. Special care is necessary in the case of light elements or in extrapolating the rules to other energies or projectiles. They have been very helpful, however, in approaching sets of parameters which give good fits with the data at 10 Mev. Any semi-empirical rules which eliminate some of the trial and error nature of this type of analysis are valuable in conserving computing time. However, the above statements are much too qualitative to yield precise fits. Instead a least-squares analysis is used which permits independent variation of three of the optical model parameters and predicts a new set of parameters which usually produces better agreement with the data. The

[18] This property has also been observed for 1-Mev neutron scattering by Feshbach, Porter, and Weisskopf.[3]

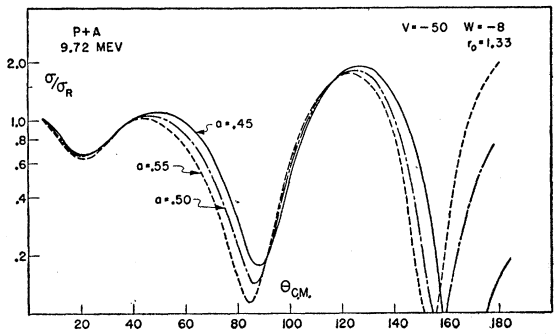

FIG. 5. Typical variation of proton-nucleus scattering with the diffuseness for medium and heavy elements. Here the main effect of increasing a is a clockwise rotation of the diffraction pattern about some value at small angles. Sometimes the changes are very much like the effects obtained by changing W illustrated in Fig. 4.

results of this procedure are illustrated in Fig. 6, where a good fit to the tin data was obtained by varying just a and W. The initial approximation used the parameters $V=-62$, $W=-8$, $r_0=1.20$, and $a=0.50$.[19] Two additional calculations were then made which gave the partial derivatives of $\sigma(\theta)/\sigma_R(\theta)$ with respect to a and W at the 35 angles from 5° to 175° in steps of 5°. In one of these, a was increased to 0.60; and in the other, W was decreased to -6. The predicted changes in these parameters, $\Delta a=0.044$ and $\Delta W=-0.95$, then produce an entirely acceptable angular distribution. The general procedure in obtaining agreement between the optical model and observed elastic proton-nucleus scattering angular distributions may be summarized as follows: Qualitative agreement is first obtained with the aid of the approximate rules stated above. Detailed fits are then achieved by a least-squares analysis. For the latter

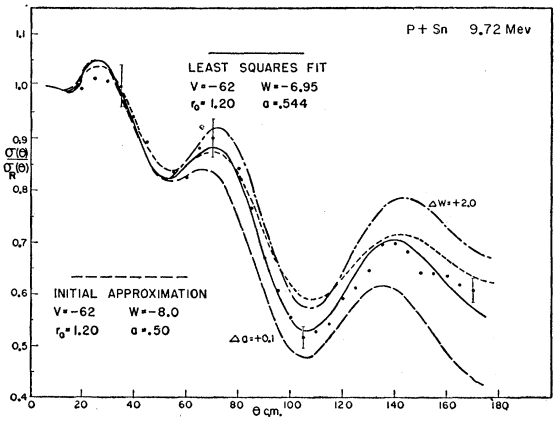

FIG. 6. Two-way least squares analysis of 9.72-Mev proton scattering from tin. After the initial approximation was made two calculations were carried out in which a was changed by 0.1 and W was changed by 2.0, permitting the derivatives of $\sigma(\theta)/\sigma_R(\theta)$ with respect to a and W to be calculated. The least squares method then yielded the solid curve which is an improved fit to the data. The bars are typical experimental errors.

[19] All energies are in Mev and lengths in 10^{-13} cm.

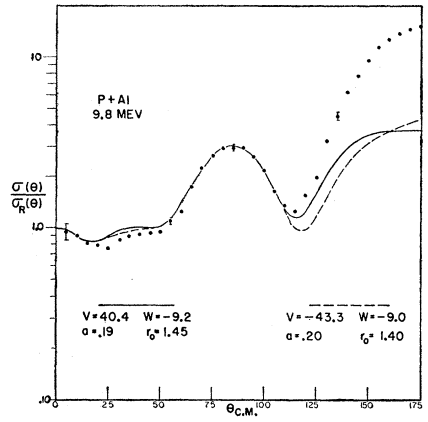

FIG. 7. Present analysis for aluminum. The two curves have in common the same value of VR^2. Other calculations with about the same values of VR^2, a, and W would work equally "well" as long as r_0 is within 5% of $r_0=1.40$. The results of this analysis are striking in that a is much smaller and r_0 somewhat larger than the other cases considered. The bars are typical experimantal errors.

to be successful, the qualitative initial approximation must not be too poor; otherwise the assumption, made by the least-squares method, of first-order changes in the parameters is violated.

III. COMPARISON WITH 9.8-MEV EXPERIMENTS

Figures 7 through 12 present the analysis of Hintz's angular distributions for protons elastically scattered from aluminum, argon, nickel, copper, and silver. The analysis of the aluminum data presented the greatest difficulty, and calculations for over 40 sets of parameters have been carried out. It is very hard to reproduce the complicated diffraction structure at forward angles less than 125° and still obtain sufficient scattering at back angles. Conversely, if the cross section is fitted at 175° (which requires a large a) the computed cross section is completely different from the data at other angles. The level of agreement achieved so far is illustrated in Fig. 7 where two typical curves with the same value of VR^2 are given. These curves were found by ignoring the data at angles greater than 125°. Agreement with the observed scattering in this sense can only be obtained by using a very small value for the diffuseness a. The values actually used are quite close to $a=0.2$, which is about 5% of the radius. This would mean a form factor which is only half as diffuse as those used for the other elements discussed here, i.e., intermediate between a square well and the diffuse wells used for the other cases. There are no other independent determinations of the surface thickness for aluminum. The electron scattering measurement for neighboring Mg^{24} is about three times as big.[4]

Since the agreement is inferior for aluminum, and since the diffuseness obtained is anomalously small, it may be that the optical model cannot be used for a nucleus with so few nucleons, at least at such low bombarding energy. On the other hand, a different form factor might be successful. Particular attention will have to be given to this case in the analysis of experiments at higher energies.

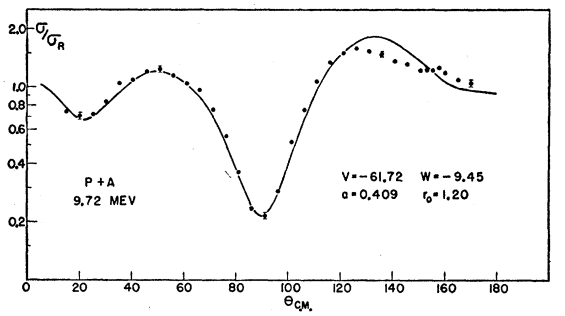

FIG. 8. Analysis for argon. Other sets of parameters with approximately the same value of VR^2, a, and W are possible but a value for r_0 as large as 1.33 is ruled out. The bars are typical experimental errors.

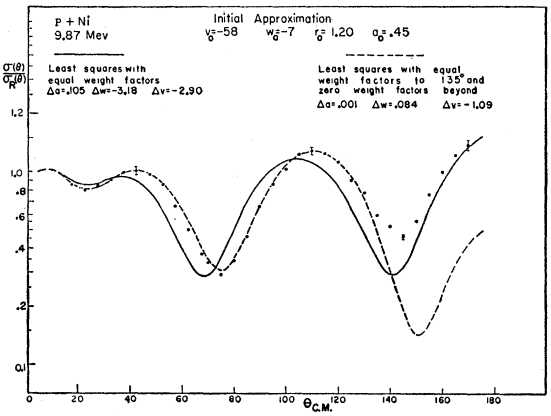

FIG. 9. Present analysis for nickel. It is possible to fit either the scattering out to the last diffraction minima or the scattering at very small and very large angles, but not both. These difficulties are in contrast to the ease with which copper may be understood. The bars are typical experimental errors.

Good agreement is obtained for argon, copper, and tin and these results are displayed in Figs. 8, 10, and 12. Once again difficulties were met in the analysis of nickel. This is of particular importance since the next element, copper, is particularly easy to fit and, in fact, allows a large range of parameters to be used. Striking differences in the scattering from neighboring elements in the region near $Z=30$ have been observed by Bromley and Wall[20,21] using 5.25-Mev protons and by Dayton and Schrank[22] using 17-Mev protons. In analyzing Hintz's data, it has been very difficult to get enough scattering beyond 135° without destroying agreement at smaller angles. This is illustrated in Fig. 9 where the same initial approximation was used to get

[20] D. A. Bromley and N. S. Wall, Phys. Rev. **99**, 1029 (1955).
[21] D. A. Bromley and N. S. Wall, Phys. Rev. **102**, 1560 (1956).
[22] I. E. Dayton and G. Schrank, Phys. Rev. **101**, 1358 (1956).

the two curves by a least squares comparison with the experimental values. For the solid curve all angles were weighted equally in the least-squares analysis and the result is agreement at back angles but nowhere else. On the other hand, if the observations beyond 135° are ignored, which is the case for the dashed curve, good agreement for angles less than 135° can easily be obtained. A rather tedious investigation which uses intermediate weight factors is now being carried out and slow progress is being made.

Hintz has observed very small deviations from Rutherford scattering for gold. They are only about 5% at large angles and are too small to be analyzed in detail. Thus only a few calculations were made for this case to insure that there was no obvious disagreement with the results for other elements. This indeed was found to be the case.

A summary of the optical model parameters at 10 Mev is presented in Table I. The stationary property

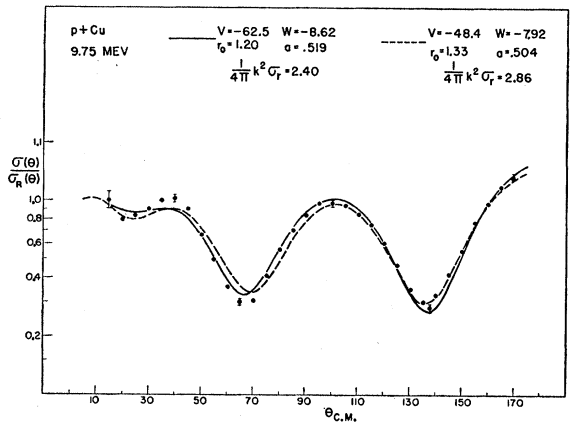

FIG. 10. Analysis for copper. Two equivalent fits are presented which have in common approximately the same value of VR^2, a, and W. Thus any radius from $r_0=1.20$ to 1.33 may be used. Smaller values are also possible but not as small as $r_0=1.10$. The bars are typical experimental errors.

of the cross-section maxima and minima obtained by keeping VR^2 fixed indicates the possibility of obtaining more than one set of acceptable parameters. In beginning the analysis for a particular element, a radius given by $r_0=1.20$ was usually used. It was then attempted to fit the observed experimental angular distribution by variation of the remaining three parameters. In other words, values of VR^2, a, and W were determined. For the three elements (argon, copper, and tin) for which good fits were obtained in this way, an investigation was made to ascertain whether V and R could be determined separately. Thus r_0 was increased to 1.33 and V was adjusted so that VR^2 remained the same. These values of V, R and the old values of a and W still provide an approximate fit, at least as far as the positions of maxima and minima are concerned. Then a and W, and V if necessary, were varied to regain agreement with experiment.

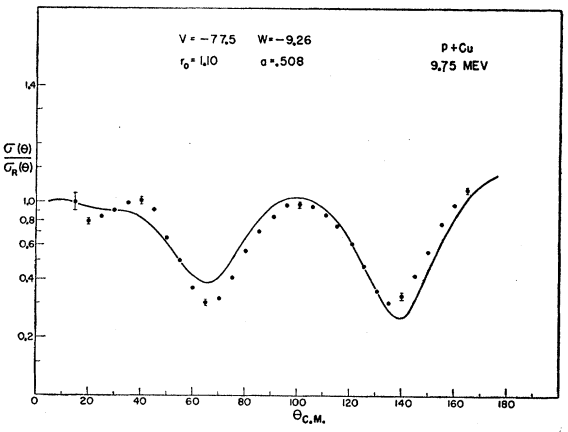

FIG. 11. Inferior agreement for copper with $r_0=1.10$. Good fits with $r_0=1.20$ and $r_0=1.33$ are given in Fig. 10. The bars are typical experimental errors.

This procedure yields the two equally good sets of parameters for copper which are given in Fig. 10. Another attempt using a very small radius with $r_0=1.10$ gives the slightly inferior fit shown in Fig. 11. An identical procedure rules out a radius as large as $r_0=1.33$ for argon and tin. However, this does not mean that $r_0=1.20$ is the only acceptable radius for these elements. Nor is it true that a radius smaller than $r_0=1.20$ or larger than $r_0=1.33$ cannot give agreement with the copper data. It is simply that a detailed investigation of the possible range of equivalent sets of parameters has not yet been made for these elements. A great deal of computing time is needed for such a project. Furthermore, it is hoped that the analysis of experiments at higher energies, which is now being carried out, will eliminate some of the solutions possible at 10 Mev, if one assumes that certain of the optical model parameters are energy-independent.

It must be emphasized that, although the two acceptable solutions for copper have nearly the same

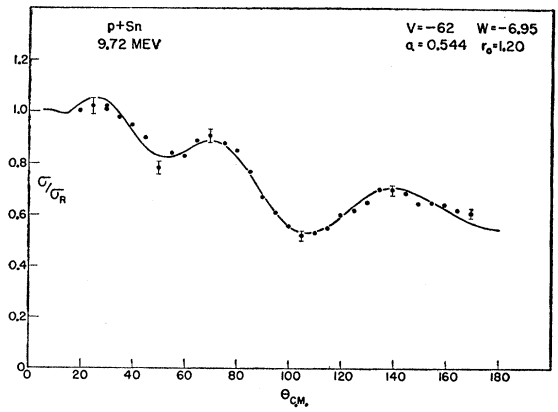

FIG. 12. Analysis for tin. Other sets of parameters with approximately the same values of VR^2, a, and W may be used but a value of r_0 as large as 1.33 is ruled out. The bars are typical experimental errors.

TABLE I. Summary of optical model parameters for 10-Mev proton-nucleus scattering. Energies are in Mev and lengths in 10^{-13} cm. These parameters are not to be considered as unique sets, and for copper equivalent sets are given. The agreement with experiments for aluminum (Fig. 7) and nickel (Fig. 9) is not as good as for the other elements. No results are listed for gold because the deviation from Rutherford scattering is too small to be analyzed.

Element	r_0	a	V	W
Al	1.45	0.19	−40.4	−9.2
A	1.20[a]	0.41	−62	−9.5
Ni	1.20	0.45	−59	−6.9
Cu	1.20[b]	0.52	−62	−8.6
Cu	1.33[b]	0.50	−48	−7.9
Sn	1.20[a]	0.54	−62	−6.9

[a] A radius as large as $r_0=1.33$ cannot be used.
[b] A radius as small as $r_0=1.10$ cannot be used.

value of VR^2, the values of a and W are not quite the same. This should not be surprising since there is no reason to believe that the four optical parameters V, W, R, and a are the *essential* parameters in this problem. For it has already been shown that VR^2 has a more direct significance than V or R alone, at least as far as the elastic scattering is concerned. Thus one should expect that, at this energy, there are probably only three important parameters and that equivalent fits to the observed angular distributions can be obtained by using a number of combinations of the four arbitrarily chosen parameters, V, W, R, and a. These sets of solutions then have in common perfectly definite values of the three essential parameters.

Table II lists the total reaction cross sections obtained in this analysis of 10-Mev proton scattering. The partial cross sections $\sigma_r^{(L)}$ for orbital angular momentum L are divided by the maximum possible cross section $(2L+1)\pi\lambda\!\!\!^{-2}$, i.e., the cross section for a black nucleus. The total cross sections are divided by the geometric cross section πR^2. For light and medium elements the reaction cross section is within 20% of this value, but for heavy elements the Coulomb barrier reduces the cross section considerably. (For scattering at 10 Mev, the energy of the incident proton is about the same or less than the Coulomb barrier.) Comparison of the reaction cross sections for the two sets of parameters consistent with the copper angular distribution shows that a measurement of the reaction could remove this ambiguity. The two solutions have reaction cross sections differing by about 20%; $\sigma_r=0.66$ barn for $r_0=1.20$ and $\sigma_r=0.79$ barn for $r_0=1.33$.

IV. BRIEF DISCUSSION OF THE OPTICAL MODEL PARAMETERS FOR 10-MEV PROTONS

One of the most important objectives of the analysis is the determination and understanding of the optical model parameters. Of particular interest are (1) the spatial distribution of the proton-nucleus interaction and a comparison with other distributions such as the nuclear charge density, and (2) the energy dependences of the strengths of the real and imaginary parts of the proton-nucleus potential and their bearing on the theory of nuclear structure. Since the present analysis deals only with 10-Mev protons, the following discussion is necessarily incomplete.

A detailed comparison of the interaction radius R is not possible until a more thorough study is made of the multiple solutions described in Sec. III, where it was shown that a number of equivalent solutions are possible which have in common approximately the same value of VR^2. Inspection of Table I shows that there is some indication that the diffuseness, a, increases with atomic weight. The electron scattering results do not show any such variation.[4] A more definite statement on this point will also have to wait until the problem of multiple solutions is resolved and until the difficulties with aluminum and nickel are better understood.

It is interesting to compare the potentials used in this analysis with the ones used for bound states, i.e., the nuclear shell model. Recently Ross, Lawson, and Mark[23] have calculated the energy levels of single-particle states in a central potential of the form used in this paper but with spin-orbit coupling of the Thomas type, and forty times stronger. Assuming a radius specified by $r_0=1.30$, the potential V, smoothing parameter a, and spin-orbit coupling strength λ, were all varied to obtain the correct level sequence. The only attempts to obtain the correct binding of the last proton as well as the last neutron were made for Au^{197} and Pb^{208}. Unfortunately the scattering of 10-Mev protons from elements as heavy as these deviates from Rutherford scattering by only about 5% at large scattering angles. Thus the optical model parameters at 10 Mev cannot be determined for these cases. However, the value of Vr_0^2 determined from scattering by elements in the middle of the periodic table shows no marked variation with A. Also Ross, Mark, and Lawson find that a neutron well which is independent of A gives good level structure and binding. Thus it seems

TABLE II. Reaction cross sections for 10-Mev proton-nucleus scattering. The total reaction cross section is divided by πR^2 and the partial cross sections are divided by the upper limit $(2L+1)\pi\lambda\!\!\!^{-2}$. The optical model parameters are given in the corresponding rows of Table I.

Element	$\sigma_r/\pi R^2$	$\sigma_r^{(0)}$	$\sigma_r^{(1)}$	$\sigma_r^{(2)}$	$\sigma_r^{(3)}$	$\sigma_r^{(4)}$
Al	1.02	0.62	0.94	0.42	0.32	0.07
A	1.23	0.89	0.64	0.83	0.17	0.11
Ni	0.85	0.99	0.53	0.59	0.17	0.06
Cu	0.92	0.85	0.77	0.62	0.38	0.06
Cu	0.89	0.94	0.75	0.76	0.45	0.03
Sn	0.39	0.58	0.65	0.36	0.19	0.04
Au[a]	0.05	0.19	0.10	0.08	0.02	0.00

[a] These cross sections were obtained with the parameters $r_0=1.20$, $a=0.50$, $V=-62$, and $W=-10$.

[23] Ross, Mark, and Lawson, Phys. Rev. **102**, 1613 (1956).

safe to extrapolate the value of Vr_0^2 for medium weight elements to very heavy elements. For a radius of $r_0=1.30$, the value of the potential is $V=-52\pm3$. The uncertainty arises from the nonsystematic variations of Vr_0^2 with A and the existence of multiple solutions which have in common only approximately the same value of Vr_0^2. In addition it should be remembered that this is an extrapolated value and that the diffuseness used in the shell-model calculations is 40% greater than in the scattering work. In any case, this value of (-52 ± 3) Mev is to be compared with -55 or -57 Mev obtained by Ross, Mark, and Lawson in the two cases considered. This comparison between the well depths for bound and unbound proton states suffers from the above uncertainties and, consequently, the apparent differences in the values of V should not be considered as significant.

The strength of the imaginary part of the nuclear potential for 10-Mev protons is in the range from -7 to -9 Mev. This corresponds to an absorption length of 5×10^{-13} cm, i.e., roughly one nuclear radius. For purposes of comparison, the absorption length for 1-Mev neutrons is 24×10^{-13} cm,[3] whereas for 20 to 40-Mev alpha particles it is about 1×10^{-13} cm.[8] The above value for W is in agreement with "frivolous" calculations[24–26] based on Goldberger's[27] model for high-energy nuclear interactions. If the only alteration made in such a calculation is the inclusion of the Coulomb repulsion for the proton inside the nucleus, the result is $W\simeq-6$ Mev. When one considers the crudeness of the method, the agreement is satisfactory.

ACKNOWLEDGMENTS

The authors are greatly indebted to Remington Rand Univac for providing the computing facilities for this research. They are also grateful to Professor J. H. Williams for his continued support and encouragement. The authors also have benefited greatly from very many discussions with Professor N. Hintz. Finally, they wish to thank Dr. P. J. Kellogg for his aid and, in particular, for whatever success has been achieved in understanding the scattering from aluminum.

APPENDIX: MATHEMATICAL PROCEDURE

In this discussion all quantities refer to the center-of-mass system, and all lengths are in units of λ. The scattering amplitude is decomposed into point-charge and nuclear parts,[28]

$$f(\theta)=-(\eta/2)\csc^2(\theta/2)\exp\{-2i[\eta\ln\sin(\theta/2)-\sigma_0]\}+\sum_L(2L+1)\exp(2i\sigma_L)C_LP_L(\cos\theta), \quad \text{(A1)}$$

where $C_L=\sin\delta_L\exp(i\delta_L)$. The total phase shift, $(\sigma_L+\delta_L)$, is also written as the sum of Coulomb and nuclear phase shifts, and $\eta=ZZ'(e^2/\hbar v)$. The coefficients C_L are determined by matching the internal and external logarithmic derivatives at a point ρ_m where the nuclear form factors, which are unity at the origin, are less than a predetermined $\epsilon_1>0$:

$$C_L=-\left(\frac{u_L'}{u_L}F_L-F_L'\right)\left[\left(\frac{u_L'}{u_L}G_L-G_L'\right)+i\left(\frac{u_L'}{u_L}F_L-F_L'\right)\right]^{-1}\Bigg|_{\rho=\rho_m}. \quad \text{(A2)}$$

The regular and irregular Coulomb functions, F_L and G_L, are those defined by Abramowitz.[29] The u_L are the solutions to the radial Schrödinger equation,

$$u_L''+[1-L(L+1)/\rho^2-V/E]u_L=0, \quad \text{(A3)}$$

which vanish at the origin.

This problem was programmed for calculation by the Univac Scientific Computer (E.R.A. 1103). The floating-point system developed at Convair provided the basic subroutines.[30] For each value of L, starting with $L=0$, Eq. (A3) was integrated numerically from an initial point h_1 close to the origin out to ρ_m. The integration subroutine[30] was Gill's version[31] of the Runge-Kutta method to solve systems of linear first-order equations. In this case, these are four equations for the real and imaginary parts of u_L and u_L'. Initial values of these functions must be specified and, to obtain the required accuracy in the logarithmic derivative, it was sufficient to use $u_L=h_1^{L+1}$ and $u_L'=(L+1)h_1^L$. The numerical integration consumed about 75% of the machine time for runs at 10 Mev and the time required for each step is about one second. A small integration step h_1 is used near the origin and where the form factor changes rapidly, i.e., in the range $kR-a<\rho<kR+a$; a larger value h_2 is used elsewhere. Typical values are $h_1=0.01$ and $h_2=0.25$.

The Coulomb functions are evaluated by an asymptotic expansion[29] especially suited for high-energy scattering. The Coulomb phase shift is also needed here as well as in Eq. (A1). For $L=0$, a slowly converging series[29] is used for $\eta\leq 2$, but for $\eta>2$ a five-term Sterling's approximation[29] gives the same accuracy; for $L>0$, recurrence relations[29] are employed. Tall-

[24] Morrison, Muirhead, and Murdoch, Phil. Mag. **46**, 795 (1955).
[25] A. M. Lane and C. F. Wandel, Phys. Rev. **98**, 1524 (1955).
[26] E. Clementel and C. Villi, Nuovo cimento **2**, 176 (1955).
[27] M. L. Goldberger, Phys. Rev. **74**, 1268 (1948).
[28] L. I. Schiff, *Quantum Mechanics* (McGraw-Hill Book Company, Inc., New York, 1949), first edition, p. 120.
[29] *Tables of Coulomb Wave Functions I*, U. S. National Bureau of Standards Applied Mathematics Series No. 17 (U. S. Government Printing Office, Washington, D. C., 1952). The introduction by M. Abramowitz contains most of the information on Coulomb functions used in this work.
[30] Flip III, Floating Point Subroutine System, Convair, Revised 1955 (unpublished).
[31] S. Gill, Proc. Cambridge Phil. Soc. **47**, 96 (1950).

qvist's six-figure table of Legendre polynomials[32] is included in the program. The entries are in intervals of 1° from 1° to 90° and for $L=0$ to $L=32$.

When the nuclear and Coulomb phase shifts are computed for a particular L, the program then adds the Lth term of the series in Eq. (A1) to the previous partial sum at every angle from 1° to 179° in 1° intervals. Unless the additional scattering from the Lth partial wave is, in relative magnitude, less than some previously prescribed $\epsilon_3>0$ at every angle, the calculation proceeds to the next value of L. Otherwise the calculation is finished and the following results are obtained: Coulomb and nuclear phase shifts for each L, the elastic scattering amplitude, the cross section, the latter's ratio to Rutherford scattering, Rutherford scattering, and the reaction cross section. In addition there are options for obtaining the results of the numerical integration and the Coulomb functions. The authors will supply any of this information to those interested upon request.

[32] H. Tallqvist, Acta Soc. Sci. Fennicae Ser. A, 2, No. 11 (1938).